Precoded and Vector OFDM Robust to Channel Spectral Nulls and With Reduced Cyclic Prefix Length in Single Transmit Antenna Systems

Xiang-Gen Xia, *Senior Member, IEEE*

***Abstract*—The performance of orthogonal frequency-division multiplexing (OFDM) systems may be degraded when intersymbol interference (ISI) channels have spectral nulls. Also, when ISI channels have many taps, the data rate overhead due to the insertion of the cyclic prefix is high. In this paper, we first propose a precoded OFDM system that may improve the performance of the OFDM systems for spectral null channels. We also propose size $K \times 1$ vector OFDM (VOFDM) systems that reduce the cyclic prefix length by K times compared to the conventional OFDM systems. The precoding scheme is simply to insert one or more zeros between each two sets of K consecutive information symbols, although it can be generalized to a general form. This precoding scheme may be able to remove the spectral nulls of an ISI channel without knowing the ISI channel. When no zero is inserted between each two sets of K consecutive information symbols and only each K consecutive symbols are blocked together, we obtain VOFDM systems. Both theoretical performance analysis and simulation results are presented. Finally, in this paper, we compare the combination of the VOFDM systems and the unitary matrix modulation with the conventional OFDM systems and the phase-shift keying modulation, where both differential (noncoherent) and coherent modulations and demodulations are considered.**

***Index Terms*—Differential en/decoding, ISI mitigation, precoded OFDM, unitary matrix modulation, vector OFDM.**

I. Introduction

ORTHOGONAL frequency-division multiplexing (OFDM) systems have been widely used in high-speed digital wireline communication systems, such as VHDSL and ADSL [3]. One of the main reasons is because OFDM systems convert intersymbol interference (ISI) channels into ISI-free channels by inserting the cyclic prefix as an overhead of the data rate at the transmitter. For tutorials, see, for example, [2], [4], and [7]. Recently, the applications of OFDM systems to high-speed digital wireless communication systems have become an active research area. In high-speed digital wireless applications, however, the ISI channel may have spectral nulls, which may degrade the performance of the existing OFDM systems because the Fourier transform of the ISI channel needs to be inverted for each subcarrier at the OFDM system receiver. For this reason, the coded OFDM systems and discrete multitone (DMT) systems were proposed in, for example, [4]–[6], where the conventional trellis-coded modulation (TCM) was used in [4] and [5], and turbo codes were used in [6]. Another problem with the existing OFDM systems is that, when the ISI channel has many taps, the data rate overhead of the cyclic prefix insertion is high.

In this paper, we first propose a precoded OFDM system by simply inserting one or more zeros between each two sets of K consecutive information symbols, which may be independent of the ISI channel. However, the precoding can be generalized to a general modulated coding (for modulated coding, see, for example [11]–[13]), where the precoding may depend on the ISI channel in an optimal way. Notice that, due to the insertion of zeros, the data rate is expanded in the precoded OFDM systems. One of the advantages of the proposed precoding scheme is that it may be able to remove the spectral nulls of an ISI channel without even knowing the channel information, which is different from the conventional OFDM (COFDM) systems [4]–[6]. The proposed precoded OFDM system does not increase the encoding/decoding complexity as much as the conventional COFDM does, where the Viterbi decoding for the conventional COFDM is needed. Another advantage of the proposed precoded OFDM system is that the cyclic prefix data rate overhead is reduced by M times compared to the one in the conventional convolutionally coded OFDM system with the same code rate K/M. Both theoretical and simulation results are presented to illustrate the theory.

We then propose VOFDM systems, which are used to reduce the data rate overhead of the prefix insertion. The basic idea for the VOFDM systems is basically from the above precoded OFDM systems, where no zeros are inserted between each two sets of K consecutive information symbols but each K consecutive information symbols are blocked together as a $K \times 1$ vector sequence. Comparing to the precoded OFDM systems, the data rate before the prefix adding for VOFDM systems is not changed. When $K \times 1$ vector sequence is processed, the ISI channel can be blocked into a $K \times K$ matrix ISI channel, but the length of the matrix ISI channel is only about $1/K$ of the original ISI channel length. The cyclic prefix length for the VOFDM system only needs to be greater than or equal to the matrix ISI channel length. This implies that the data rate overhead of the original cyclic prefix insertion is reduced by K times for the VOFDM systems. The bit-error rate (BER) performances of the

Paper approved by Y. Li, the Editor for Wireless Communications Theory of the IEEE Communications Society. Manuscript received May 18, 1999; revised May 10, 2000 and October 15, 2000. This work was supported in part by the Air Force Office of Scientific Research (AFOSR) under Grant F49620-00-1-0086, the National Science Foundation CAREER Program under Grant MIP-9703377, and the University of Delaware Research Foundation. This paper was presented in part at the International Conference on Communications, New Orleans, LA, June 2000.

The author is with the Department of Electrical and Computer Engineering, University of Delaware, Newark, DE 19716 USA (e-mail: xxia@ee.udel.edu).

Publisher Item Identifier S 0090-6778(01)06934-3.

vector and conventional OFDM systems are compared. Our simulation results show that the BER performance of the VOFDM systems is comparable to the one of the conventional OFDM systems.

The **main idea** for the above studies is simple. In the conventional OFDM systems, the scalar ISI channel is converted to N scalar ISI-free subchannels. In the proposed precoded or vector OFDM systems, scalar sequences are vectorized, and a scalar ISI channel is converted to a matrix ISI channel. Furthermore, the proposed OFDM systems convert the matrix ISI channel into N matrix ISI-free subchannels with N constant matrices (no ISI across the N matrix subchannels). These N constant matrices can be squared or not. The precoded OFDM systems in this paper correspond to the nonsquared case while the VOFDM systems correspond to the squared case.

It should be emphasized that the precoded and vector OFDM systems proposed in this paper are for single antenna [single-input and single-output (SISO)] systems, which are different from those for multiple antenna [multi-input multi-output (MIMO)] systems [8]–[10], [19]. However, since SISO systems are blocked into MIMO systems, the proposed OFDM system equations at the receiver in this paper have similar forms as in [8]–[10].

Finally, in this paper we compare the combination of the VOFDM system and the unitary matrix modulation with the conventional OFDM system and the phase-shift keying (PSK) modulation. Both differential (noncoherent) and coherent modulations/demodulations are considered. The unitary matrix modulation proposed in this paper is motivated from the space–time coding and modulation recently proposed in [20]–[25] where multiple antennas are used, while in this paper a single antenna is used. The combined space–time coding and the MIMO-OFDM systems have appeared in [9] and [27], and space–time code design in OFDM systems has appeared in [26].

This paper is organized as follows. In Section II, the conventional OFDM system and its performance analysis are reviewed. In Section III, a general precoded OFDM system is introduced with a general formulation. In Section IV, we study the precoded OFDM system, which is the one we want to propose for the robustness of the spectral null channels. In Section V, we study the VOFDM system. The OFDM systems in Sections IV and V can be thought of as special cases of the OFDM systems proposed in Section III. In Section VI, we study the combination of the vector and precoded OFDM and the unitary matrix modulation. In Section VII, simulation and theoretical results are presented to illustrate the theory.

II. Brief Review of the Uncoded OFDM Systems

In this section, the conventional OFDM systems are briefly reviewed including the theoretical bit-error rate (BER) performance analysis.

Let $x(n)$ stand for the information symbol sequences after the binary to complex mapping, such as binary PSK (BPSK) and quadrature PSK (QPSK) symbol sequences. Let N be the number of carriers in the OFDM system, i.e., the size of the inverse fast Fourier transform (IFFT) and fast Fourier transform

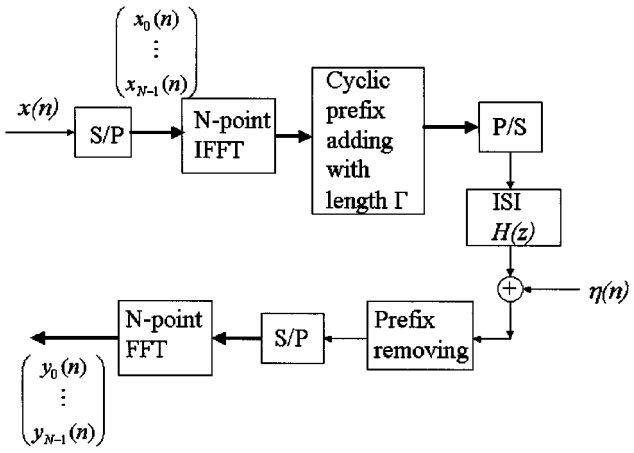

Fig. 1. Conventional OFDM system.

(FFT) in the OFDM system as shown in Fig. 1 is N. Let the ISI channel have the following transfer function:

$$H(z) = \sum_{n=0}^{L} h(n) z^{-n} \tag{2.1}$$

where $h(n)$ are the impulse responses of the ISI channel. Let Γ be the cyclic prefix length in the OFDM system as shown in Fig. 1 and $\Gamma \geq L$ for the purpose of removing the ISI. Let $\eta(n)$ be the additive white Gaussian noise (AWGN), as shown in Fig. 1, with mean zero and variance $\sigma^2 = N_0/2$ and N_0 is the single-sided power spectral density of the noise $\eta(n)$. Let $r(n)$ be the received signal at the receiver and $y(n)$ be the signal after the FFT of the received signal $r(n)$. Then, the relationship between the information symbols $x(n)$ and the signal $y(n)$ can be formulated as

$$y_k(n) = H_k x_k(n) + \xi_k(n), \qquad k = 0, 1, \ldots, N-1 \tag{2.2}$$

where $q_k(n)$ denotes the kth subsequence of $q(n)$, i.e., $(q(n))_n = (q_0(n), q_1(n), \ldots, q_{N-1}(n))_n$, and q stands for x, y, and $\xi, \xi(n)$ is the FFT of the noise $\eta(n)$ and therefore has the same statistics as $\eta(n)$, and

$$H_k = H(z)|_{z=\exp(j2\pi k/N)}, \qquad k = 0, 1, \ldots, N-1. \tag{2.3}$$

The receiver needs to detect the information sequence $x_k(n)$ from $y_k(n)$ through (2.2).

From (2.2), one can clearly see that the ISI channel $H(z)$ is converted to N ISI-free subchannels H_k. The *key* for this property to hold is the insertion of the cyclic prefix with length Γ that is greater than or equal to the the number of ISI taps L. Similar property will be used in the following precoded OFDM systems in Section III.

For the ISI-free system in (2.2), the performance analysis of the detection is as follows. Let $P_{\mathrm{ber},x}(E_\mathrm{b}/N_0)$ be the BER for the signal constellation $x(n)$ in the AWGN channel at the signal-to-noise ratio (SNR) E_b/N_0, where E_b is the energy per bit. Then, the BER versus E_b/N_0 of the OFDM shown in Fig. 1 is

$$P_\mathrm{e} = \frac{1}{N} \sum_{k=0}^{N-1} P_{\mathrm{ber},x}\left(\frac{|H_k|^2 N E_\mathrm{b}}{(N+\Gamma)N_0}\right). \tag{2.4}$$

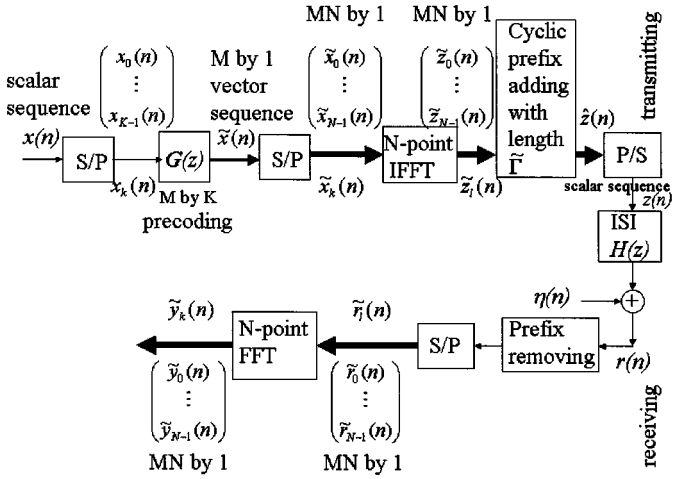

Fig. 2. Precoded OFDM system.

For example, when the BPSK for $x(n)$ is used, we have

$$P_{\mathrm{ber},x}\left(\frac{E_\mathrm{b}}{N_0}\right) = Q\left(\sqrt{\frac{2E_\mathrm{b}}{N_0}}\right). \tag{2.5}$$

Therefore, the BER versus E_b/N_0 for the OFDM system is

$$P_\mathrm{e} = \frac{1}{N}\sum_{k=0}^{N-1} Q\left(\sqrt{\frac{2|H_k|^2 N E_\mathrm{b}}{(N+\Gamma)N_0}}\right). \tag{2.6}$$

Numerical examples will be presented in Section VII.

III. General Precoded OFDM Systems

We now propose a precoded OFDM system whose block diagram is shown in Fig. 2. It is formulated as follows, which is the goal of this section.

A. System Description

Symbol $x(n)$ is as before, the information sequence after the binary to complex mapping. The information sequence $x(n)$ is blocked into $K \times 1$ vector sequence

$$\bar{x}(n) = (x_0(n), x_1(n), \ldots, x_{K-1}(n))^\mathrm{T}$$

where $^\mathrm{T}$ denotes the transpose and $x_k(n) = x(Kn+k)$, $k = 0, 1, \ldots, K-1$.

Symbol $G(z)$ is a precoder and an $M \times K$ polynomial matrix, i.e., $G(z) = (g_{ij}(z))_{M\times K}$, where $g_{ij}(z)$, in general, is a polynomial of z^{-1}.

The precoded $M \times 1$ vector sequence is denoted by $\tilde{x}(n)$. Let $K \times 1$ polynomial vector $\bar{X}(z)$ and $M \times 1$ polynomial vector $\tilde{X}(z)$ denote the z transforms of vector sequences $\bar{x}(n)$ and $\tilde{x}(n)$, respectively. Then

$$\tilde{X}(z) = G(z)\bar{X}(z). \tag{3.1}$$

The precoded $M \times 1$ vector sequence $\tilde{x}(n)$ is *blocked again* into $MN \times 1$ vector sequence

$$\hat{x}(n) = \left(\tilde{x}_0^\mathrm{T}(n), \tilde{x}_1^\mathrm{T}(n), \ldots, \tilde{x}_{N-1}^\mathrm{T}(n)\right)^\mathrm{T}$$

where each $\tilde{x}_k(n) = \tilde{x}(Nn+k)$ is already an $M \times 1$ vector for $k = 0, 1, \ldots, N-1$.

Let $\tilde{z}_l(n)$, $l = 0, 1, \ldots, N-1$, be the output of the N-point IFFT of $\tilde{x}_k(n)$, $k = 0, 1, \ldots, N-1$, i.e.,

$$\tilde{z}_l(n) = \frac{1}{\sqrt{N}}\sum_{k=0}^{N-1}\tilde{x}_k(n)\exp\left(\frac{j2\pi kl}{N}\right), \qquad l = 0, 1, \ldots, N-1 \tag{3.2}$$

which is the N-point IFFT of the individual components of the N vectors $\tilde{x}_k(n)$.

The cyclic prefix in Fig. 2 is to add the first $\tilde{\Gamma}$ vectors $\tilde{z}_l(n)$, $l = 0, 1, \ldots, \tilde{\Gamma}-1$, to the end of the vector sequence $\tilde{z}_l(n)$, $l = 0, 1, \ldots, N-1$. In other words, the vector sequence after the cyclic prefix is

$$\hat{z}(n) = \left(\tilde{z}_0^\mathrm{T}(n), \tilde{z}_1^\mathrm{T}(n), \ldots, \tilde{z}_{N-1}^\mathrm{T}(n), \tilde{z}_0^\mathrm{T}(n), \ldots, \tilde{z}_{\tilde{\Gamma}-1}^\mathrm{T}(n)\right)^\mathrm{T} \tag{3.3}$$

which has size $M(N+\tilde{\Gamma}) \times 1$. The cyclic prefix length $\tilde{\Gamma}$ will be determined later for the purpose of removing the ISI of the precoded OFDM system. Notice that each subvector $\tilde{z}_l(n)$ in $\hat{z}(n)$ in (3.3) has size $M \times 1$ and the prefix components are also vectors rather than scalars in the conventional OFDM systems as shown in Fig. 1.

The transmitted scalar sequence in the precoded OFDM system in Fig. 2 is $z(n)$ that is obtained by the parallel to serial conversion of the vector sequence $\hat{z}(n)$ in (3.3). Notice that the precoded OFDM system in Fig. 2 is different from the OFDM systems with antenna diversities, such as [8]–[10]. In the precoded OFDM system in Fig. 2, there is only *one* transmitting antenna and *one* receiving antenna.

$r(n)$ is the received scalar sequence at the receiver, which is converted to the following $MN \times 1$ vector sequence

$$\hat{r}(n) = \left(\tilde{r}_0^\mathrm{T}(n), \tilde{r}_1^\mathrm{T}(n), \ldots, \tilde{r}_{N-1}^\mathrm{T}(n)\right)^\mathrm{T}$$

where each $\tilde{r}_l(n)$ has size $M \times 1$. The output of the N-point FFT of $\hat{r}(n)$ is

$$\tilde{y}_k(n) = \frac{1}{\sqrt{N}}\sum_{l=0}^{N-1}\tilde{r}_l(n)\exp\left(\frac{-j2\pi lk}{N}\right), \qquad k = 0, 1, \ldots, N-1 \tag{3.4}$$

where the formulation is similar to the N-point IFFT in (3.2) and each $\tilde{y}_k(n)$ is an $M \times 1$ vector.

B. An Example

Let us see an example to illustrate the above scheme. Consider a four-tap ISI channel $(h(0), h(1), h(2), h(3))$, i.e., $L = 3$. Consider precoder

$$G(z) = G = \begin{bmatrix} 1 & 0 \\ 0 & 1 \\ 0 & 0 \end{bmatrix}$$

where $M = 3$ and $K = 2$. Consider $N = 4$ point IFFT and FFT in the OFDM system.

Suppose the information to transmit is

$$\big(x(0),x(1),x(2),x(3),x(4),x(5),x(6),x(7),x(8),\\ x(9),x(10),x(11),x(12),x(13),x(14),x(15)\big).$$

First, it is blocked into a vector sequence of vector size $K=2$ and then the vector sequence is blocked again with block length $N=4$ by the serial to parallel conversion shown in the equation at the bottom of the page.

Then, the blocked vector sequence is precoded into a 3×1 vector sequence by multiplying the precoder G to it, as shown in (3.5) at the bottom of the page.

Then, take the four-point IFFT of $\tilde{\mathbf{x}}_\mathbf{0},\tilde{\mathbf{x}}_\mathbf{1},\tilde{\mathbf{x}}_\mathbf{2},\tilde{\mathbf{x}}_\mathbf{3},\tilde{\mathbf{x}}_\mathbf{4}$, and $\tilde{\mathbf{x}}_\mathbf{5}$ and obtain a new 3×1 vector sequence, shown in the equation, below (3.5), at the bottom of the page.

Next, vector cyclic prefixs of length $\tilde{\Gamma}=\tilde{L}=L/M=3/3=1$ for the above two blocks

$$\begin{bmatrix}\tilde{z}(9)\\ \tilde{z}(10)\\ 0\end{bmatrix}\quad\text{and}\quad\begin{bmatrix}\tilde{z}(21)\\ \tilde{z}(22)\\ 0\end{bmatrix}$$

respectively, are added to the above vector sequence as shown in the last equation at the bottom of the page.

Finally, we rearrange the above vector sequence $\{\tilde{z}(n)\}$ by the parallel-to-serial conversion into a scalar sequence $z(n)$

$$\{z(n)\}=\big(\tilde{z}(9)\tilde{z}(10)0\tilde{z}(0)\tilde{z}(1)0\tilde{z}(3)\tilde{z}(4)0\tilde{z}(6)\tilde{z}(7)0\\ \tilde{z}(9)\tilde{z}(10)0\tilde{z}(21)\tilde{z}(22)0\tilde{z}(12)\tilde{z}(13)0\tilde{z}(15)\\ \tilde{z}(16)0\tilde{z}(18)\tilde{z}(19)0\tilde{z}(21)\tilde{z}(22)0\big)$$

which is transmitted through a single antenna.

At the receiver, the received signal $r(n)$ is represented as

$$r(n)=z(n)*h(n)+\eta(n),\qquad n=0,2,\ldots,Q-1$$

where $Q=M\times(N+\tilde{\Gamma})\times 2+L=3\times(4+1)\times 2+3=33$, $*$ is the convolution, and $\eta(n)$ is the additive noise.

Before taking the FFT, the vector cyclic prefixs are removed. After the cyclic prefixs are removed and the serial-to-parallel conversion, we have the top equation shown at the bottom of the next page, where the prefixes $r(0),r(1),r(2),r(15),r(16),r(17)$, and $r(30),r(31),r(32)$ are deleted for the ISI removal as we shall see later.

By taking the four-point FFT of $\tilde{\mathbf{r}}$, we have the last equation shown at the bottom of the page. Finally, $\{\tilde{y}(n)\}$ is used for the decoding as we shall see later in (4.6).

C. Matrix Input and Output Equation

In what follows, we want to derive the similar output and input relationship between $\tilde{y}_k(n)$ and $\tilde{x}_k(n)$ as in (2.2) for converting the ISI channel into an ISI-free channel, where and also in what follows "ISI-free" means that there is no interference between intervectors.

Since an SISO linear time-invariant (LTI) system with transfer function $H(z)$ is equivalent to an M input and M output system by the blocking process with block length M, i.e., the serial-to-parallel process. The equivalence here means that the M inputs and M outputs are the blocked versions (or serial to parallel conversions) of the SISO and vice versa. The equivalent systems are shown in Fig. 3, where the equivalent MIMO transfer function matrix $\mathcal{H}(z)$ is the blocked version of $H(z)$ and is given by the following pseudocirculant polynomial

$$\begin{bmatrix}\mathbf{x_0} & \mathbf{x_2}\\ \mathbf{x_1} & \mathbf{x_3}\end{bmatrix}=\left[\begin{array}{cccc:cccc}x(0)&x(2)&x(4)&x(6)&x(8)&x(10)&x(12)&x(14)\\ x(1)&x(3)&x(5)&x(7)&x(9)&x(11)&x(13)&x(15)\end{array}\right]$$

$$\begin{bmatrix}\tilde{\mathbf{x}}_\mathbf{0} & \tilde{\mathbf{x}}_\mathbf{3}\\ \tilde{\mathbf{x}}_\mathbf{1} & \tilde{\mathbf{x}}_\mathbf{4}\\ \tilde{\mathbf{x}}_\mathbf{2} & \tilde{\mathbf{x}}_\mathbf{5}\end{bmatrix}=G\begin{bmatrix}\mathbf{x_0} & \mathbf{x_3}\\ \mathbf{x_1} & \mathbf{x_3}\end{bmatrix}=\begin{bmatrix}1&0\\0&1\\0&0\end{bmatrix}\begin{bmatrix}\mathbf{x_0} & \mathbf{x_3}\\ \mathbf{x_1} & \mathbf{x_3}\end{bmatrix}=\begin{bmatrix}\mathbf{x_0} & \mathbf{x_3}\\ \mathbf{x_1} & \mathbf{x_3}\\ \mathbf{0} & \mathbf{0}\end{bmatrix}=\left[\begin{array}{cccc:cccc}x(0)&x(2)&x(4)&x(6)&x(8)&x(10)&x(12)&x(14)\\ x(1)&x(3)&x(5)&x(7)&x(9)&x(11)&x(13)&x(15)\\ 0&0&0&0&0&0&0&0\end{array}\right] \tag{3.5}$$

$$\begin{bmatrix}\tilde{\mathbf{z}}_\mathbf{0} & \tilde{\mathbf{z}}_\mathbf{3}\\ \tilde{\mathbf{z}}_\mathbf{1} & \tilde{\mathbf{z}}_\mathbf{4}\\ \tilde{\mathbf{z}}_\mathbf{2} & \tilde{\mathbf{z}}_\mathbf{5}\end{bmatrix}=\begin{bmatrix}\mathrm{IFFT}(\tilde{\mathbf{x}}_\mathbf{0}) & \mathrm{IFFT}(\tilde{\mathbf{x}}_\mathbf{3})\\ \mathrm{IFFT}(\tilde{\mathbf{x}}_\mathbf{1}) & \mathrm{IFFT}(\tilde{\mathbf{x}}_\mathbf{4})\\ \mathrm{IFFT}(\tilde{\mathbf{x}}_\mathbf{2}) & \mathrm{IFFT}(\tilde{\mathbf{x}}_\mathbf{5})\end{bmatrix}=\left[\begin{array}{cccc:cccc}\tilde{z}(0)&\tilde{z}(3)&\tilde{z}(6)&\tilde{z}(9)&\tilde{z}(12)&\tilde{z}(15)&\tilde{z}(18)&\tilde{z}(21)\\ \tilde{z}(1)&\tilde{z}(4)&\tilde{z}(7)&\tilde{z}(10)&\tilde{z}(13)&\tilde{z}(16)&\tilde{z}(19)&\tilde{z}(22)\\ 0&0&0&0&0&0&0&0\end{array}\right].$$

$$\{\tilde{z}(n)\}=a\begin{bmatrix}\hat{\mathbf{z}}_\mathbf{0} & \hat{\mathbf{z}}_\mathbf{3}\\ \hat{\mathbf{z}}_\mathbf{1} & \hat{\mathbf{z}}_\mathbf{4}\\ \hat{\mathbf{z}}_\mathbf{2} & \hat{\mathbf{z}}_\mathbf{5}\end{bmatrix}=\left[\begin{array}{ccccc:cccc}\tilde{z}(9)&\tilde{z}(0)&\tilde{z}(3)&\tilde{z}(6)&\tilde{z}(9)&\tilde{z}(21)&\tilde{z}(12)&\tilde{z}(15)&\tilde{z}(18)&\tilde{z}(21)\\ \tilde{z}(10)&\tilde{z}(1)&\tilde{z}(4)&\tilde{z}(7)&\tilde{z}(10)&\tilde{z}(22)&\tilde{z}(13)&\tilde{z}(16)&\tilde{z}(19)&\tilde{z}(22)\\ 0&0&0&0&0&0&0&0&0&0\end{array}\right].$$

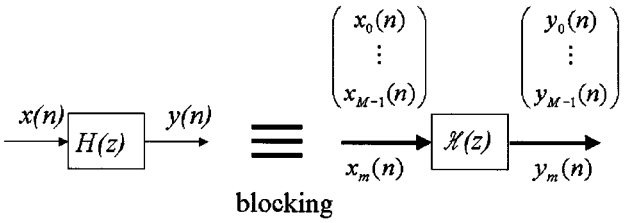

Fig. 3. Equivalent SISO and MIMO systems.

matrix (see [14] and [16])

$$\mathcal{H}(z)=\begin{bmatrix} h_0(z) & z^{-1}h_{M-1}(z) & \cdots & z^{-1}h_1(z) \\ h_1(z) & h_0(z) & \cdots & z^{-1}h_2(z) \\ \vdots & \vdots & \vdots & \vdots \\ h_{M-2}(z) & h_{M-3}(z) & \cdots & z^{-1}h_{M-1}(z) \\ h_{M-1}(z) & h_{M-2}(z) & \cdots & h_0(z) \end{bmatrix} \tag{3.6}$$

where $h_k(z)$ is the kth polyphase component of $H(z)$, i.e.,

$$h_k(z)=\sum_l h(Ml+k)z^{-l}, \qquad k=0,1,\ldots,M-1.$$

If the order of $H(z)$ is L as in (2.1), then the order $\tilde{L}$ of the blocked version $\mathcal{H}(z)$ in (3.6) of $H(z)$ with block size M is

$$\tilde{L}=\left\lceil \frac{L}{M} \right\rceil \tag{3.7}$$

where $\lceil a \rceil$ stands for the smallest integer b such that $b \geq a$. Clearly

$$\tilde{L}<\frac{L}{M}+1. \tag{3.8}$$

Using the above equivalence of the SISO and MIMO systems, the precoded OFDM system in Fig. 2 is equivalent to the one shown in Fig. 4. The equivalent precoded OFDM system in Fig. 4 is the same as the conventional OFDM system in Fig. 1 if the scalar sequences $x(n)$ and $y(n)$ are replaced by $M \times 1$ vector sequences $\tilde{x}(n)$ and $\tilde{y}(n)$, respectively. Therefore, similar to (2.2), it is not hard to derive the relationship between $\tilde{x}_k(n)$ and $\tilde{y}_k(n)$

$$\tilde{y}_k(n)=\mathcal{H}_k\tilde{x}_k(n)+\tilde{\xi}_k(n), \qquad k=0,1,\ldots,N-1 \tag{3.9}$$

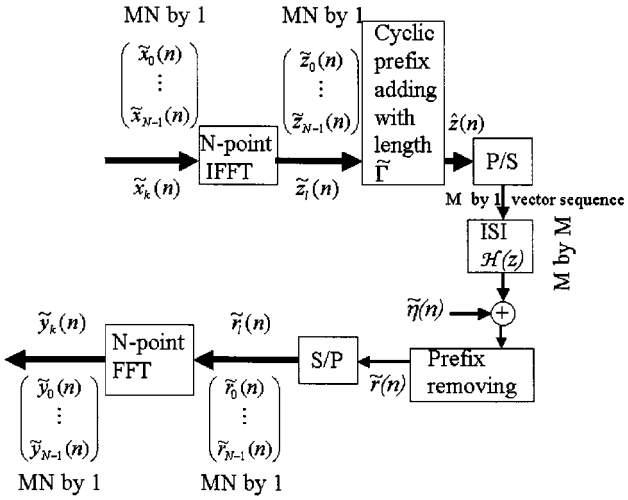

Fig. 4. An equivalent precoded OFDM system.

under the condition on the cyclic prefix length $\tilde{\Gamma}$ that should be greater than or equal to the order of the MIMO transfer function matrix $\mathcal{H}(z)$ in (3.6), i.e.,

$$\tilde{\Gamma} \geq \tilde{L}. \tag{3.10}$$

The constant matrices $\mathcal{H}_k$ in (3.9) are similar to the constants H_k in (2.2) and have the following forms:

$$\mathcal{H}_k=\mathcal{H}(z)|_{z=\exp(j2\pi k/N)}, \qquad k=0,1,\ldots,N-1. \tag{3.11}$$

The additive noise $\tilde{\xi}_k(n)$ in (3.9) is the blocked version of $\xi(n)$ and its components have the same power spectral density as $\eta(n)$ does and all components of all the vectors $\tilde{\xi}_k(n)$ are independently, identically distributed complex Gaussian random variables in general.

IV. Precoded OFDM Systems

The goal of this section is to restrict ourselves to a special precoding scheme that is independent of the ISI channel $H(z)$.

A. A Special Precoder

Before going to the details, we first see the rationale. By noticing that the vector sequence $\tilde{x}_k(n)$ in (3.9) is the precoded sequence of the original information sequence $x_k(n)$ in Fig. 2,

$$\{\tilde{r}(n)\}=\begin{bmatrix} \tilde{\mathbf{r}}_\mathbf{0} & \tilde{\mathbf{r}}_\mathbf{3} \\ \tilde{\mathbf{r}}_\mathbf{1} & \tilde{\mathbf{r}}_\mathbf{4} \\ \tilde{\mathbf{r}}_\mathbf{2} & \tilde{\mathbf{r}}_\mathbf{5} \end{bmatrix}=\left[\begin{array}{cccc:cccc} r(3) & r(6) & r(9) & r(12) & r(18) & r(21) & r(24) & r(27) \\ r(4) & r(7) & r(10) & r(13) & r(19) & r(22) & r(25) & r(28) \\ r(5) & r(8) & r(11) & r(14) & r(20) & r(23) & r(26) & r(29) \end{array}\right]$$

$$\{\tilde{y}(n)\}=\begin{bmatrix} \mathrm{FFT}(\tilde{\mathbf{r}}_\mathbf{0}) & \mathrm{FFT}(\tilde{\mathbf{r}}_\mathbf{3}) \\ \mathrm{FFT}(\tilde{\mathbf{r}}_\mathbf{1}) & \mathrm{FFT}(\tilde{\mathbf{r}}_\mathbf{4}) \\ \mathrm{FFT}(\tilde{\mathbf{r}}_\mathbf{2}) & \mathrm{FFT}(\tilde{\mathbf{r}}_\mathbf{5}) \end{bmatrix}=\left[\begin{array}{cccc:cccc} \tilde{y}_1(0) & \tilde{y}_1(3) & \tilde{y}_1(6) & \tilde{y}_1(9) & \tilde{y}_2(0) & \tilde{y}_2(3) & \tilde{y}_2(6) & \tilde{y}_2(9) \\ \tilde{y}_1(1) & \tilde{y}_1(4) & \tilde{y}_1(7) & \tilde{y}_1(10) & \tilde{y}_2(1) & \tilde{y}_2(4) & \tilde{y}_2(7) & \tilde{y}_2(10) \\ \tilde{y}_1(2) & \tilde{y}_1(5) & \tilde{y}_1(8) & \tilde{y}_1(11) & \tilde{y}_2(2) & \tilde{y}_2(5) & \tilde{y}_2(8) & \tilde{y}_2(11) \end{array}\right].$$

there are two methods for detecting the original information sequence $x_k(n)$. One method is to detect $\tilde{x}_k(n)$ first from the ISI-free vector system (3.9) and then decode the precoder $G(z)$ for $x_k(n)$. The problem with this method is that, when the ISI channel $H(z)$ is spectral null, the blocked matrix channel $\mathcal{H}(z)$ is also spectral null by the following diagonalization of $\mathcal{H}(z^M)$ (see [15] and [16]):

$$\mathcal{H}(z^M) = (\mathbf{W}_M^* \Lambda(z))^{-1} \operatorname{diag}\big(H(z), H(zW_M), \ldots, H\left(zW_M^{M-1}\right)\big) \mathbf{W}_M^* \Lambda(z) \tag{4.1}$$

where $W_M = \exp(-j2\pi/M)$ and $\mathbf{W}_M$ is the discrete Fourier transform (DFT) matrix of size M, i.e., $\mathbf{W}_M = (W_M^{mn})_{0\le m,n\le M-1}$ and $\Lambda(z) = \operatorname{diag}(1, z^{-1}, \ldots, z^{-M+1})$. One will see later that the performance of the detection of $\tilde{x}_k(n)$ in (3.9) for spectral null ISI channels is too poor that the coding gain of the precoder $G(z)$ is far away to make it up. This implies that the separate ISI removing and precoder decoding may not perform well for spectral null channels, which is similar to the existing COFDM systems.

The other method is the joint ISI removing and precoder decoding, i.e., the combination of the precoder $G(z)$ with the vector systems (3.9). If the precoder $G(z)$ is not a *constant matrix*, the encoded vector sequence $\tilde{x}_k(n)$ is the convolution of the information vector sequence $x_k(n)$ and the precoder impulse response $g(n)$. The convolution and the constant matrix $\mathcal{H}_k$ multiplications in (3.9) induces ISI, which may complicate the decoding of the system (3.9) and is beyond the scope of this paper.

The above arguments suggest that we may want to use a constant $M \times K$ matrix precoder $G(z) = G$. In this case, (3.9) becomes

$$\tilde{y}_k(n) = \mathcal{H}_k G \bar{x}_k(n) + \tilde{\xi}_k(n), \qquad k = 0, 1, \ldots, N-1 \tag{4.2}$$

where for $k = 0, 1, \ldots, N-1$

$$\begin{aligned} \bar{x}_k(n) &= \bar{x}(Nn+k) \\ &= (x_0(Nn+k), x_1(Nn+k), \ldots, x_{K-1}(Nn+k))^{\mathrm{T}} \\ &= (x(K(Nn+k)+0), x(K(Nn+k)+1), \ldots, \\ &\quad x(K(Nn+k)+K-1))^{\mathrm{T}} \end{aligned} \tag{4.3}$$

are the original $K \times 1$ information vector sequences and need to be detected from $\tilde{y}_k(n)$. It is clear that one wants to have the singular values of all matrices $\{\mathcal{H}_k G\}_{k=0,1,\ldots,N-1}$ as large as possible for the optimal output SNR. However, since the transmitter usually does not have the channel information $\mathcal{H}_k$, it may not be easy to optimally design the constant precoder G in (4.2) at the transmitter. The above two arguments suggest the study of the following precoder.

In what follows, we use the following simplest precoder G:

$$G(z) = G = \begin{bmatrix} I_{K\times K} \\ 0_{(M-K)\times K} \end{bmatrix} \tag{4.4}$$

where $M > K$, $I_{K\times K}$ stands for the $K \times K$ identity matrix and $0_{(M-K)\times K}$ stands for $(M-K) \times K$ all-zero matrix. The precoder (4.4) is just inserting $M-K$ zeros between each two sets of K consecutive information samples. This precoder was first used in [11] for converting a spectral null channel into a nonspectral-null matrix channel as long as the M equally spaced rotations of the zero set of $H(z)$ do not intersect each other. Notice that the precoder (4.4) is independent of the ISI channel and does not change the signal energy, i.e., the energy of the signal $x(n)$ before the precoding is equal to the energy of the signal $\tilde{x}(n)$ after the precoding.

When the precoder (4.4) is used, the input-output ISI-free system (4.2) can be rewritten as follows. For each k, let $\bar{\mathcal{H}}_k$ denote the first K column submatrix of $\mathcal{H}_k$, i.e.,

$$\begin{aligned} &\text{if} \quad \mathcal{H}_k = (h_{mn})_{0\le m\le M-1, 0\le n\le M-1} \quad \text{then} \\ &\qquad \bar{\mathcal{H}}_k = (h_{mn})_{0\le m\le M-1, 0\le n\le K-1}. \end{aligned} \tag{4.5}$$

Therefore

$$\tilde{y}_k(n) = \bar{\mathcal{H}}_k \bar{x}_k(n) + \tilde{\xi}_k(n), \qquad k = 0, 1, \ldots, N-1 \tag{4.6}$$

where $\bar{x}_k(n)$ is as (4.3). Notice that the same system as (4.6) was obtained in [8]–[10] for multiple antenna systems, while in this paper only one antenna is used.

As mentioned before, without the data rate expansion, i.e., $M = K$ in (4.4), the above system (4.6) may not be invertible if the ISI channel $H(z)$ has spectral nulls, i.e., $\mathcal{H}_k$ may not be invertible (may have zero singular values). We, however, will study this case later for the purpose of reducing the prefix length rather than improving the robustness of the system. With the data rate expansion, i.e., $M > K$, it was proved in [11] that, under a minor condition on the channel as mentioned before, the nonsquared matrices $\bar{\mathcal{H}}_k$ are invertible (have all nonzero singular values). Clearly, the performance of the detection of the information symbols $\bar{x}_k(n)$ in (4.6) depends on how large the singular values of the $M \times K$ matrices $\bar{\mathcal{H}}_k$ are, i.e., how high the output SNR is. From the above argument, the precoding is already able to convert systems $\mathcal{H}_k$ with possibly zero singular values into systems $\bar{\mathcal{H}}_k$ with all nonzero singular values. From this point of view, intuitively the precoding may improve the performance of the OFDM system. We next want to show a simple example to analytically see how the precoding improves the performance.

B. An Example

We now consider a simple example to see how the precoding works. Let the ISI channel be

$$H(z) = \frac{1}{\sqrt{2}}(1 + z^{-1}).$$

Consider four carriers, i.e., $N = 4$, and $1/2$ rate precoder (4.4), i.e., $K = 1$ and $M = 2$. In this case, the precoding inserts one zero in each two information symbols. According to (3.6), the blocked ISI channel with block size 2 is

$$\mathcal{H}(z) = \frac{1}{\sqrt{2}} \begin{bmatrix} 1 & z^{-1} \\ 1 & 1 \end{bmatrix}. \tag{4.7}$$

In the conventional OFDM system, the input-output relationship (2.2) is

$$y_k(n) = \frac{1}{\sqrt{2}}\left(1+\exp\left(\frac{-j2\pi k}{4}\right)\right)x_k(n)+\xi_k(n), \quad k=0,1,2,3 \tag{4.8}$$

where $H_k = 1+\exp(-j2\pi k/4)/\sqrt{2}$ or $H_0 = \sqrt{2}$, $H_1 = 1-j/\sqrt{2}$, $H_2 = 0$, and $H_3 = 1+j/\sqrt{2}$. One can see that the third subcarrier channel in (4.8) completely fails. The BER performance of the conventional OFDM system is, thus

$$P_{\rm e} \approx \frac{1}{4}\frac{1}{2} = \frac{1}{8}. \tag{4.9}$$

For the precoded OFDM system, the input-output relationship (4.6) is

$$\tilde{y}_k(n) = \frac{1}{\sqrt{2}}\begin{bmatrix}1\\1\end{bmatrix}x_k(n)+\tilde{\xi}_k(n), \qquad k=0,1,2,3 \tag{4.10}$$

where

$$\bar{\mathcal{H}}_k = \frac{1}{\sqrt{2}}\begin{bmatrix}1\\1\end{bmatrix}, \qquad k=0,1,2,3$$

which have the same singular value 1. Equation (4.10) is rewritten as

$$\frac{1}{\sqrt{2}}[1\ \ 1]\tilde{y}_k(n) = x_k(n)+\tilde{\xi}'_k(n) \tag{4.11}$$

where $\tilde{\xi}'_k(n)$ are complex Gaussian random variables with the same statistics as $\tilde{\xi}_k(n)$. In this case, the BER performance of the precoded OFDM is the same as the uncoded AWGN performance if the additional cyclic prefix is ignored. For example, when BPSK is used, the BER is

$$P_{\rm e} = Q\left(\sqrt{\frac{2E_{\rm b}}{N_0}}\right). \tag{4.12}$$

As a remark, since the precoder (4.4) does not increase the signal energy, the bit energy $E_{\rm b}$ before the prefix insertion does not increase although the data rate is increased. In (4.12), the cyclic prefix data expansion is ignored otherwise the $E_{\rm b}/N_0$ in (4.12) needs to be replaced by

$$\frac{NE_{\rm b}}{(N+\tilde{\Gamma})N_0} = \frac{4E_{\rm b}}{5N_0}.$$

Clearly, the BER performance (4.12) of the precoded OFDM system is much better than (4.9) of the uncoded OFDM system. To increase the data rate for our precoded OFDM system, high rate modulation schemes, such as 4QAM or 6QAM, can be used before the precoded OFDM system. The **key** reason for the improvement is that the precoded OFDM systems here may erase the spectral nulls as shown in the above simple example, where the spectral null characteristics plays the key role in the performance degradation of an OFDM system. We shall see more complicated and general examples later via computer simulations.

Let us consider the precoder (4.4) without data rate increase, i.e., $M = K$. In this case, the input-output relationship (4.2) for the precoded OFDM system, which will be called VOFDM later, becomes

$$\tilde{y}_k(n) = \frac{1}{\sqrt{2}}\begin{bmatrix}1 & {\rm e}^{-j2\pi k/4}\\ 1 & 1\end{bmatrix}\bar{x}_k(n)+\tilde{\xi}_k(n), \qquad k=0,1,2,3 \tag{4.13}$$

where

$$\mathcal{H}_k = \frac{1}{\sqrt{2}}\begin{bmatrix}1 & {\rm e}^{-j2\pi k/4}\\ 1 & 1\end{bmatrix}, \qquad k=0,1,2,3$$

and the singular values of $\mathcal{H}_0$ are $\sqrt{2}$ and 0, which confirms the previous argument, i.e., the zero singular value cannot be removed if no data rate expansion is used in the precoding. In this case, there are equivalently eight subchannels and one of them fails due to the 0 singular value. Thus, the BER performance is

$$P_{\rm e} \approx \frac{1}{8}\frac{1}{2} = \frac{1}{16}. \tag{4.14}$$

Notice that, even when a subchannel fails, the BER performance (4.14) of the VOFDM system is better than the one (4.9) of the conventional OFDM system. This will be seen in Section VI from other simulation results for all other examples presented in this paper.

We next derive the analytical BER versus $E_{\rm b}/N_0$ for the precoded OFDM systems for general ISI channels.

C. Performance Analysis of the Precoded OFDM Systems

To study the BER performance of the precoded OFDM systems proposed in Section IV-A, let us go back to the MIMO system (4.6), where the components of the vectors $\bar{x}_k(n)$ defined in (4.3) are from the original information symbols $x(n)$. We need to estimate $\bar{x}_k(n)$ from $\tilde{y}_k(n)$ through (4.6) for each fixed index k. There are different methods for the estimation, such as the maximum-likelihood (ML) estimation and the least square (LS) estimation. In what follows, for the BER performance analysis, we use the LS estimation, which is simpler. For the simulations presented in Section VI, we use the ML estimation for each fixed index k. Clearly, the BER for the LS estimation is an upper bound of the BER for the ML estimation when the vector size of $\bar{x}_k(n)$ is greater than 1, i.e., $K > 1$.

The LS estimator of $\bar{x}_k(n)$ in (4.6) is given by

$$\hat{\bar{x}}_k(n) = (\bar{\mathcal{H}}_k)^{\dagger}\tilde{y}_k(n), \qquad k=0,1,\ldots,N-1 \tag{4.15}$$

where † stands for the pseudoinverse, i.e.,

$$(\bar{\mathcal{H}}_k)^{\dagger} = \left((\bar{\mathcal{H}}_k^*)^{\rm T}\bar{\mathcal{H}}_k\right)^{-1}(\bar{\mathcal{H}}_k^*)^{\rm T}. \tag{4.16}$$

The noise of the LS estimator $\hat{\bar{x}}_k(n)$ is

$$\hat{\tilde{\xi}}_k(n) = (\bar{\mathcal{H}}_k)^{\dagger}\tilde{\xi}_k(n) \tag{4.17}$$

whose components are, in general, complex Gaussian random variables but may not be white. Then, the theoretical BER can be calculated as long as the original binary to complex mapping, number of carriers N, the ISI channel $H(z)$, and the precoding rate K/M are given.

For simplicity, let us consider the BPSK signal constellation. In this case, the complex Gaussian random noise are reduced to the real Gaussian random noise by cutting the imaginary part

that does not affect the performance. Thus, the noise in this case is

$$\mathrm{Re}(\hat{\tilde{\xi}}_{\mathrm{k}}(\mathrm{n})).$$

Therefore, the BER versus E_{b}/N_0 for the LS estimator given in (4.15) is

$$P_{\mathrm{e}} = \frac{2^{K-1}}{2^K-1}\frac{1}{N} \cdot \sum_{k=0}^{N-1}\left(1-\frac{1}{(2\pi)^{K/2}(\det M_k)^{1/2}} \cdot \int_{-\gamma_{\mathrm{b}}}^{\infty}\cdots\int_{-\gamma_{\mathrm{b}}}^{\infty}\exp\left\{-\frac{1}{2}\bar{x}^{\mathrm{T}}M_k^{-1}\bar{x}\right\}dx_1\cdots dx_K\right) \tag{4.18}$$

where the factor $2^{K-1}/(2^K-1)$ is due to the conversion of the symbol-error rate (SER) of $\bar{x}$ to the BER, $\bar{x}=(x_1,\ldots,x_K)$

$$\gamma_{\mathrm{b}} = \sqrt{\frac{2E_{\mathrm{b}}N}{N_0(N+\tilde{\Gamma})}} \tag{4.19}$$

and

$$M_k = \mathrm{Re}\left((\bar{\mathcal{H}}_{\mathrm{k}})^{\dagger}\right)\mathrm{Re}\left((\bar{\mathcal{H}}_{\mathrm{k}})^{\dagger}\right)^{\mathrm{T}} + \mathrm{Im}\left((\bar{\mathcal{H}}_{\mathrm{k}})^{\dagger}\right)\mathrm{Im}\left((\bar{\mathcal{H}}_{\mathrm{k}})^{\dagger}\right)^{\mathrm{T}}. \tag{4.20}$$

The overall data rate overhead can be easily calculated as

$$\frac{M(N+\tilde{\Gamma})}{KN} \approx \frac{M(N+\frac{L}{M})}{KN} = \frac{MN+L}{KN} \tag{4.21}$$

where $L+1$ is the length of the ISI channel $H(z)$, and $\approx$ is due to the fact that $\tilde{\Gamma}=\lceil L/M\rceil = L/M$ if L is a multiple of M and $1+L/M$ otherwise. The uncoded OFDM systems reviewed in Section II correspond to the case when $K=M=1$, in which the data rate overhead for the uncoded OFDM systems is

$$\frac{N+L}{N}. \tag{4.22}$$

From (4.21), the data rate overhead for the cyclic prefix insertion in the precoded OFDM is $L/(KN)$. Let us consider a conventional convolutionally coded OFDM with the same code rate K/M. The overall data rate in this is

$$\frac{M(N+\Gamma)}{KN} = \frac{M(N+L)}{KN} = \frac{MN+ML}{KN}. \tag{4.23}$$

Thus, the data rate overhead for the cyclic prefix is $ML/(KN)$, which is M times more than the one in the precoded OFDM.

V. Vector OFDM Systems

When the ISI channel length $L+1$ in (2.1) is large, the cyclic prefix length $\Gamma=L$ in the conventional OFDM systems is large too. As a consequence, the data rate overhead $(N+L)/N$ is high when L is large. In this section, we propose VOFDM systems that reduce the data rate overhead while the ISI channels are still converted to ISI-free channels.

The VOFDM systems are the precoded systems in Fig. 2 with the special precoder $G(z)=I_{K\times K}$ that basically blocks the input data into $K\times 1$ vectors and the data rate is not changed, i.e., no redundancy is added. In other words, the precoder (4.4) in the precoded OFDM systems takes the squared identity matrix, i.e., $M=K$ in (4.4). Similar to (4.21), the vector cyclic prefix data rate overhead is

$$\frac{K(N+\tilde{\Gamma})}{KN} \approx \frac{N+\frac{L}{K}}{N}. \tag{5.1}$$

Comparing to the data rate overhead $(N+L)/N$ for the conventional OFDM systems, the data rate overhead in the VOFDM systems is reduced by K times, where K is the vector size.

The receiver is the same as the one for the precoded OFDM systems in Section IV-A and IV-C with $K=M$. In this case, the ISI-free systems (4.6) at the receiver becomes

$$\tilde{y}_k(n) = \mathcal{H}_k\bar{x}_k(n) + \tilde{\xi}_k(n), \qquad k=0,1,\ldots,N-1 \tag{5.2}$$

where $\mathcal{H}_k$ are defined in (3.11) and (3.6). As mentioned in the preceding sections, the robustness of the VOFDM systems to spectral nulls of ISI channels is similar to the one of the conventional uncoded OFDM systems, since no redundancy is inserted in VOFDM systems. In other words, the BER performance of the VOFDM systems is similar to the one for the uncoded OFDM systems. From our simulations, the performance of the VOFDM systems is comparable to the one of the uncoded OFDM systems (see Figs. 7–9). The performance analysis in Section IV-C for the precoded OFDM systems applies to the VOFDM systems by replacing $M=K$.

As a remark, to reduce the cyclic prefix overhead, another simple way is to increase the number N of the subcarriers, i.e., the DFT/IDFT size, in the conventional OFDM system. In the above VOFDM, the prefix overhead is reduced the same as this simple way, but the DFT/IDFT size does not increase.

VI. Combination With Unitary Matrix Modulation

In this section, we first study the combination of the VOFDM and the unitary matrix modulation.

In Fig. 1, the binary to complex mapping is implemented before the input, i.e., the input $x(n)$ is already after the mapping and complex-valued scalar sequence. For convenience, let us consider the VOFDM system first. The VOFDM combined with the unitary matrix modulation is shown in Fig. 5. The mapping is done on the $K\times 1$ vector binary vector sequence $\tilde{s}(n)=(s_0(n),s_1(n),\ldots,s_{K-1}(n))^{\mathrm{T}}$. Let 2^P distinct $K\times K$ unitary matrices be $U_0,U_1,\ldots,U_{2^P-1}$ with $(U_l^*)^{\mathrm{T}}U_l=I_K$ for $0\le l\le 2^P-1$ and $2^P\ge 2^{K^2}$. The $K\times K$ unitary matrix modulation in Fig. 5 has two different forms. One is the *coherent unitary matrix modulation*, where the channel is assumed known at the receiver as studied in [20]–[22] for space–time coding. The other is the *differential unitary matrix modulation*, where the channel is not known at the receiver as studied in [24] and [25] for differential space–time modulation.

The coherent unitary matrix modulation in Fig. 5 is the following one-to-one mapping $\mathcal{P}$ between binary $K\times K$ matrices

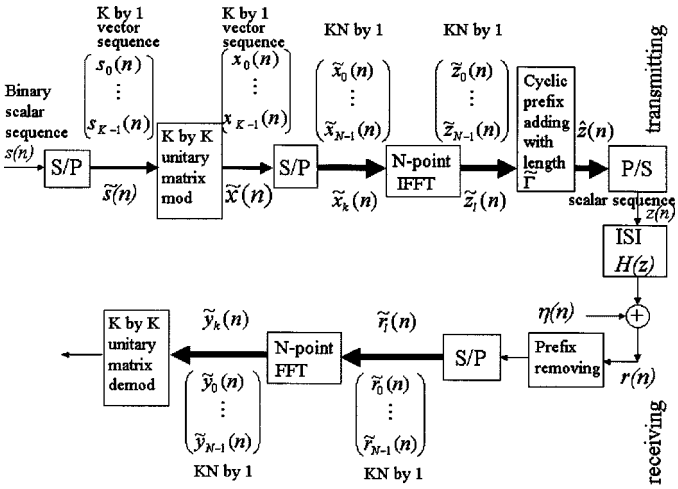

Fig. 5. VOFDM with unitary matrix modulation.

and $U_0, U_1, \ldots, U_{2^P-1}$, given in (6.1), shown at the bottom of the page, where $x_k(n)$ is the same as those in Fig. 5.

The differential unitary matrix modulation in Fig. 5 is

$$\tilde{\mathbf{x}}(0) = I_{K\times K} \tag{6.2}$$

$$\tilde{\mathbf{x}}(n) = \mathcal{P}(\tilde{\mathbf{s}}(n))\tilde{\mathbf{x}}(n-1), \qquad n = 1, 2, \ldots \tag{6.3}$$

where the notations $\tilde{\mathbf{s}}(n), \tilde{\mathbf{x}}(n)$ and the mapping $\mathcal{P}$ are the same as in (6.1).

There are two remarks we want to make here as follows.

Remark 1: The unitary matrix size of U_l in the modulation does not have to be the same as the one of the input binary matrices, i.e., K, in Fig. 4. Basically, it can be any positive integer.

Remark 2: The combination of the precoded OFDM with the special precoder G in (4.4) with the unitary matrix modulation is similar to the above VOFDM case as follows. Let the unitary matrices U_l of size $K\times K$ for convenience. The vector sequence $\tilde{x}(n)$ in Fig. 5 is then of the following form:

$$\tilde{\mathbf{x}}(n) = \begin{bmatrix} U_l \\ \mathbf{0} \end{bmatrix} \tag{6.4}$$

where $\mathbf{0}$ is the all-zero matrix of size $(M-K)\times K$. The vector sizes, $KN \times 1$, in Fig. 5 become $MN \times 1$.

At the receiver, the input and output relationship (4.6) after the prefix removing and the DFT still holds. By grouping the input and output vectors into matrices, (4.6) becomes

$$\tilde{\mathbf{y}}_k(n) = \tilde{\mathcal{H}}_k \bar{\mathbf{x}}_k(n) + \Xi_k(n) \tag{6.5}$$

where $\tilde{\mathbf{y}}_k(n) = (\tilde{y}_k(Kn-K+1), \ldots, \tilde{y}_k(Kn-1), \tilde{y}_k(Kn))$ is of size $M\times K$, $\bar{\mathbf{x}}_k(n) = (\bar{x}_k(Kn-K+1), \ldots, \bar{x}_k(Kn-1), \bar{x}_k(Kn))^{\mathrm{T}}$ is of size $K\times K$, and $\Xi_k(n) = (\tilde{\xi}_k(Kn-K+1), \ldots, \tilde{\xi}_k(Kn-1), \tilde{\xi}_k(Kn))$ is of size $M\times K$ for each $k, 0 \le k \le N-1$.

Going back to Section III-A, the difference between $M\times 1$ vector sequence $\tilde{x}(n)$ and $K\times 1$ vector sequence $\bar{x}(n)$ is that $\tilde{x}(n)$ is the output of the precoding of the information data $\bar{x}(n)$ as in (3.1) in general. In the VOFDM case, these two are equal, i.e., $\tilde{x}(n) = \bar{x}(n)$.

Note that in the coherent unitary matrix modulation, $\bar{\mathbf{x}}_k(n)$ is one of the 2^P unitary matrices U_l, and in the differential unitary matrix modulation it is one of the products of these unitary matrices. The coherent and differential unitary matrix demodulation in Fig. 5 are the same as the coherent and the differential space–time demodulations studied in [20]–[22], [24], and [25], respectively.

VII. Numerical Results

In this section, we present numerical results for some theoretical and simulation curves of the BER versus E_b/N_0 for the precoded and vector OFDM systems using conventional modulations and unitary matrix modulations. In the VOFDM, the vector size $M = K = 2$. Comparing to the BPSK OFDM case, the number of unitary matrices is $2^4 = 16$, i.e., in the unitary matrix modulation, a 2×2 binary matrix is mapped to one of 16 2×2 unitary matrices. The 16 2×2 unitary matrices used in the following simulations are from [28] for $l = 0, 1, \ldots, 15$:

$$U_l = \begin{bmatrix} \exp\left(\frac{jl\pi}{8}\right) & 0 \\ 0 & \exp\left(\frac{j3l\pi}{8}\right) \end{bmatrix} \begin{bmatrix} \cos\left(\frac{l\pi}{2}\right) & \sin\left(\frac{l\pi}{2}\right) \\ -\sin\left(\frac{l\pi}{2}\right) & \cos\left(\frac{l\pi}{2}\right) \end{bmatrix} \times \begin{bmatrix} \exp\left(\frac{jl\pi}{4}\right) & 0 \\ 0 & \exp\left(\frac{-jl\pi}{4}\right) \end{bmatrix}. \tag{7.1}$$

$$\begin{aligned} \tilde{\mathbf{s}}(n) &\triangleq (\tilde{s}(Kn-K+1), \ldots, \tilde{s}(Kn-1), \tilde{s}(Kn)) \\ &= \begin{bmatrix} s_0(Kn-K+1) & \cdots & s_0(Kn-1) & s_0(Kn) \\ s_1(Kn-K+1) & \cdots & s_1(Kn-1) & s_1(Kn) \\ \cdots & \cdots & \cdots & \cdots \\ s_{K-1}(Kn-K+1) & \cdots & s_{K-1}(Kn-1) & s_{K-1}(Kn) \end{bmatrix} \\ &\longrightarrow \mathcal{P}(\tilde{\mathbf{s}}(n)) \\ &= U_l = \begin{bmatrix} x_0(Kn-K+1) & \cdots & x_0(Kn-1) & x_0(Kn) \\ x_1(Kn-K+1) & \cdots & x_1(Kn-1) & x_1(Kn) \\ \cdots & \cdots & \cdots & \cdots \\ x_{K-1}(Kn-K+1) & \cdots & x_{K-1}(Kn-1) & x_{K-1}(Kn) \end{bmatrix} \\ &\triangleq \tilde{\mathbf{x}}(n), \qquad 0 \le l \le 2^P - 1 \end{aligned} \tag{6.1}$$

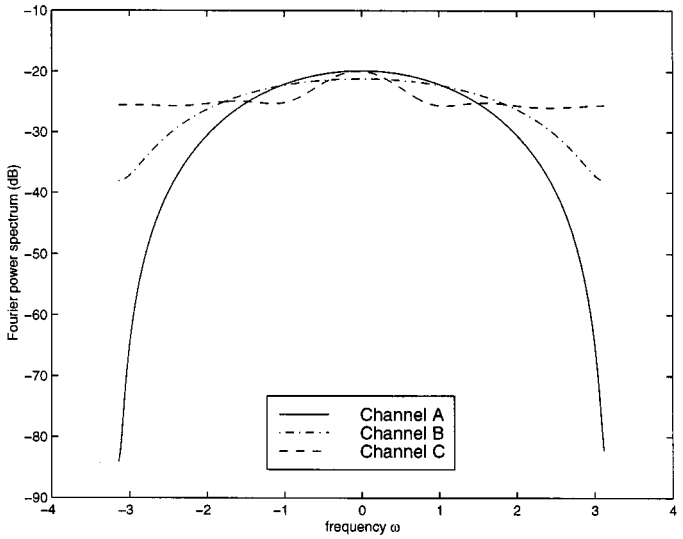

Fig. 6. Fourier spectrum for three ISI channels.

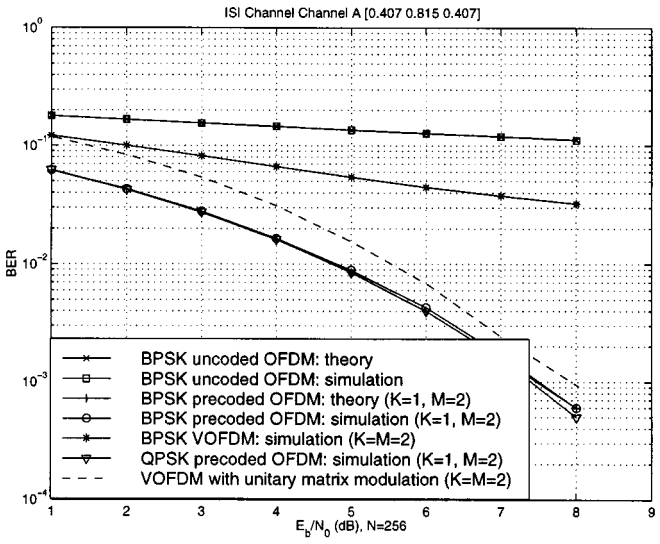

Fig. 7. Performance comparison for OFDM systems: Channel A.

This code has the best product diversity in the literature of the same size, which is $2^{1/4}/2$ following the notation in [24].

We first consider the following three fixed ISI channels.

Channel A: $h = [0.407, 0.815, 0.407]$, which is a spectral-null channel.

Channel B: $h = [0.8, 0.6]$, which, although, does not have spectral-nulls, its Fourier transform values at some frequencies are small and the small values cause the performance of the conventional uncoded OFDM system.

Channel C: $h = [0.0001 + 0.0001j,\ 0.0485 + 0.0194j,\ 0.0573 + 0.0253j,\ 0.0786 + 0.0282j,\ 0.0874 + 0.0447j,\ 0.9222 + 0.3031j,\ 0.1427 + 0.0349j,\ 0.0835 + 0.0157j,\ 0.0621 + 0.0078j,\ 0.0359 + 0.0049j,\ 0.0214 + 0.0019j]$, which does not have spectral null or small Fourier transform values.

The number of carriers is $N = 256$ in the simulations for these three fixed channels. Their Fourier power spectrum (decibels) are plotted in Fig. 6. Channel A and Channel C are selected from the examples presented in [17].

For Channel A and Channel B, six curves of the BER versus E_b/N_0 are plotted in Figs. 7 and 8, respectively. The theoretical and simulated curves for the uncoded OFDM system with BPSK signaling are marked by $\times$ and $\square$, respectively. The theoretical and simulated curves for the precoded OFDM system with rate $1/2$, i.e., $K = 1$ and $M = 2$, and the BPSK signaling are marked by $+$ and $\circ$, respectively. The simulated curve for the precoded OFDM system with rate $1/2$, i.e., $K = 1$ and $M = 2$, and the QPSK signaling is marked by ∇. One can clearly see the improvement of the precoding. The BER performances of the uncoded and precoded OFDM systems are incomparable. The QPSK precoded OFDM system has the same data rate as the uncoded BPSK OFDM system, while their performances are much different.

From Fig. 6, the nonspectral-null property of Channel B is better than the one of Channel A. One can see that the BER performances of all the OFDM systems in Fig. 8 for Channel B are better than the ones in Fig. 7 for Channel A. Notice that the

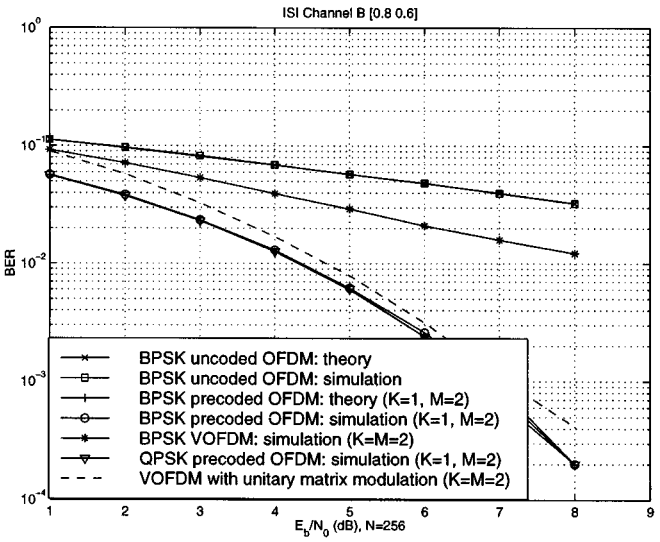

Fig. 8. Performance comparison for OFDM systems: Channel B.

performance in Fig. 7 for Channel A is better than the one of the conventional equalization techniques, such as MMSE-DFE, in a single-carrier system (see [17, p. 297, Fig. 6.12]).

The curves for the VOFDM with vector size $K = 2$, i.e., $K = M = 2$ in the precoded OFDM system are marked by $*$ in Figs. 7 and 8. One can see that the performance for the VOFDM system is comparable to the one for the uncoded OFDM system for this two channels. The data rate overhead for Channel A is saved by half for the VOFDM system comparing with the conventional OFDM system.

For Channel C, three simulation curves of the BER versus E_b/N_0 are plotted in Fig. 9, where the signal constellations are all BPSK. The uncoded conventional OFDM system is marked by $\circ$. The precoded OFDM system of rate $1/2$ with $K = 1$ and $M = 2$ is marked by ∇. The VOFDM system with vector size 2, i.e., $K = M = 2$, is marked by $+$. Since the ISI channel is not spectral null, the precoding does not show too much performance advantage. The cyclic prefix data rate overhead for the

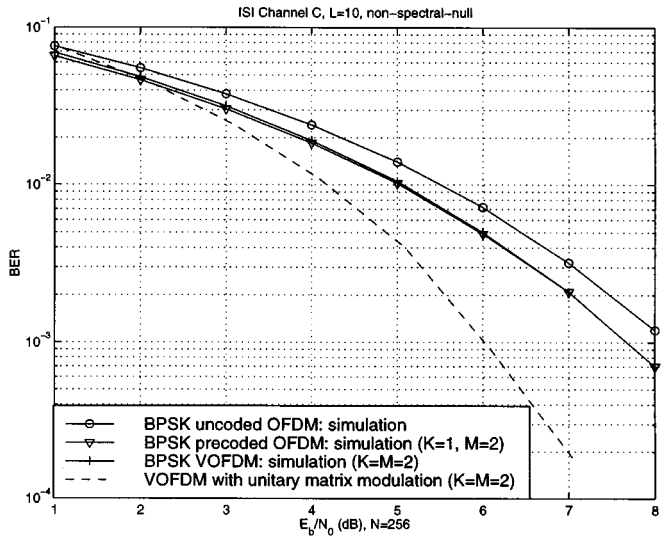

Fig. 9. Performance comparison for OFDM systems: Channel C.

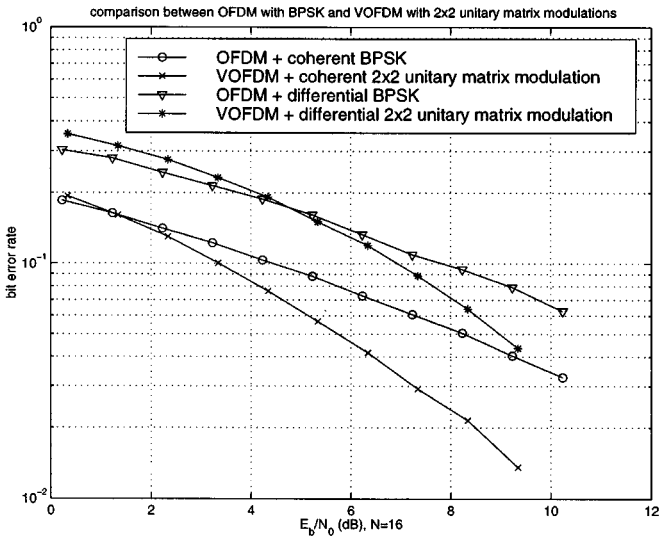

Fig. 10. Performance comparison between the BPSK OFDM and the VOFDM with unitary matrix modulation of 16 2×2 unitary matrices for nonfixed ISI channels of length 12: both coherent and differential modulations.

VOFDM is $5/256$ and the one for the conventional OFDM is $10/256$, where the prefix length is reduced by half.

The dashed lines in Figs. 7–9 show the curves of the BER versus E_b/N_0 of the VOFDM with coherent unitary matrix modulations for the three ISI channels, respectively, where the channels are known and the coherent demodulation is used at the receiver. One can see that they are better than both conventional OFDM and VOFDM systems with BPSK signaling.

We next consider another simulation for nonfixed ISI channels and VOFDM with both coherent and differential modulations. In this simulation, the number of carriers is $N = 16$ for the simulation convenience in averaging over the ISI channels. The length of ISI channels is randomly chosen as 2, i.e., $L = 11$. The cyclic prefix data rate overhead for the conventional OFDM and the VOFDM are $11/16$ and $6/16$, respectively. The ISI channels randomly change according to the Rayleigh distribution every 0 bits once and they do not change in 0 bit lengths. Fig. 10 shows both coherent and differential modulation schemes, where in the coherent case the ISI channel is known and the coherent demodulation is used at the receiver and in the differential case the ISI channel is unknown and the noncoherent demodulation is used at the receiver. From Fig. 10, one can see that the combined VOFDM with unitary matrix modulation outperforms the conventional BPSK OFDM. The complexity is, however, significantly higher since the decision of one of 16 unitary matrices in (7.1) is needed, while in the BPSK case the decision of one of two is needed.

VIII. Conclusion

In this paper, we proposed a novel precoding method for the OFDM and a novel VOFDM for single antenna systems, where the precoding does not depend on the ISI channel. The precoding is simply to insert one or more zeros between two sets of K consecutive information symbols. Unlike the existing COFDM systems, the precoded OFDM systems proposed in this paper basically erases the spectral nulls of an ISI channel. The data rate loss in the precoded OFDM because of the precoding can be remedied by using higher signal constellations, for instance, changing the BPSK to the QPSK. Furthermore, compared to the one in the conventional convolutionally coded OFDM system with the same code rate K/M, the cyclic prefix data rate overhead in the proposed precoded OFDM system is reduced M times. Theoretical and simulation results were presented. The VOFDM systems proposed in this paper are able to reduce the cyclic prefix data rate overhead for the conventional OFDM systems by K times, where K is the vector size. We numerically showed that the performance of the VOFDM systems is comparable to the one of the conventional OFDM systems. This precoding scheme has been recently analyzed in Rayleigh fading wireless communication systems in [18].

In this paper, we also studied the combination of the precoded and VOFDM with the unitary matrix modulation in both coherent and differential (noncoherent) cases. Some numerical comparisons between this scheme and the conventional BPSK OFDM were made. From the numerical simulations, we found that the VOFDM with unitary matrix modulation in both coherent and differential cases outperforms the conventional OFDM and the VOFDM with BPSK signaling.

For spectral null channels, an obvious way to erase the spectral nulls by coding is that no information symbols is sent at the null frequencies. This coding method may improve the performance. However, because this coding depends on where the spectral nulls of the ISI channel are, the transmitter needs to know the ISI channel, which may be not possible in some applications. The precoding proposed in this paper is channel independent. On the other hand, the number of zeros inserting between information symbols may have the impact on the performance for different ISI channels. As mentioned in the Introduction, the precoded OFDM systems can be generalized to general modulated coded OFDM systems with general $G(z)$ in Fig. 2. The optimal design of such precoders is under our current investigations in both cases of known and unknown ISI channels.

REFERENCES

[1] L. J. Cimini, "Analysis and simulation of a digital mobile channel using orthogonal frequency division multiple access," *IEEE Trans. Commun.*, vol. COM-33, pp. 665–675, July 1985.

[2] J. A. C. Bingham, "Multicarrier modulation for data transmission: An idea whose time has come," *IEEE Commun. Mag.*, vol. 28, pp. 4–14, May 1990.

[3] P. S. Chow, J. C. Tu, and J. M. Cioffi, "Performance evaluation of a multichannel transceiver system for ADSL and VHDSL services," *IEEE J. Select. Areas Commun*, vol. 9, pp. 909–919, Aug. 1991.

[4] W. Y. Zou and Y. Wu, "COFDM: A review," *IEEE Trans. Broadcast.*, vol. 41, pp. 1–8, Mar. 1995.

[5] T. N. Zogakis, J. T. Aslanis Jr, and J. M. Cioffi, "A coded and shaped discrete multitone system," *IEEE Trans. Commun.*, vol. 43, pp. 2941–2949, Dec. 1995.

[6] B. L. Floch, M. Alard, and C. Berrou, "Coded orthogonal frequency division multiplex," *Proc. IEEE*, vol. 83, pp. 982–996, June 1995.

[7] A. N. Akansu, O Duhamel, X. Liu, and M. de Courville, "Orthogonal transmultiplexers in communications: A review," *IEEE Trans. Signal Processing*, vol. 46, pp. 979–995, Apr. 1998.

[8] Y. Li. and N. R. Sollenberger, "Adaptive antenna arrays for OFDM systems with cochannel interference," *IEEE Trans. Commun.*, vol. 47, pp. 217–229, Feb. 1999.

[9] Y. Li, N. Seshadri, and S. Ariyavisitakul, "Channel estimation for OFDM systems with transmitter diversity in mobile wireless channels," *IEEE J. Select. Areas Commun.*, vol. 17, pp. 461–471, Mar. 1999.

[10] Y. Li, J. Chuang, and N. R. Sollenberger, "Transmitter diversity for OFDM systems and its impact on high-rate wireless networks," *IEEE J. Select. Areas Commun.*, vol. 17, pp. 1233–1243, July 1999.

[11] X.-G. Xia, "New precoding for intersymbol interference cancellation using nonmaximally decimated multirate filterbanks with ideal FIR equalizers," *IEEE Trans. Signal Processing*, vol. 45, pp. 2431–2441, Oct. 1997.

[12] X.-G. Xia, P. Fan, and Q. Xie, "A new coding scheme for ISI channels: Modulated codes," in *Proc. Int. Conf. Communications.*, Vancouver, BC, Canada, June 6–10, 1999.

[13] X.-G. Xia, "A new coded zero-forcing decision feedback equalizer using modulated codes," in *Proc. MILCOM*, Atlantic City, NJ, Oct. 31–Nov. 3, 1999.

[14] S. K. Mitra and R. Gnanasekaran, "Block implementation of recursive digital filters-New structures and properties," *IEEE Trans. Circuits Syst.*, vol. CAS-25, pp. 200–207, Apr. 1978.

[15] P. P. Vaidyanathan and S. K. Mitra, "Polyphase networks, block digital filtering, LPTV systems, and alias-free QMF banks: a unified approach based on pseudocirculants," *IEEE Trans. Signal Processing*, vol. 36, pp. 381–391, Mar. 1988.

[16] P. P. Vaidyanathan, *Multirate Systems and Filter Banks*. Englewood Cliffs, NJ: Prentice-Hall, 1993.

[17] G. L. Stuber, *Principles of Mobile Communication*. Boston, MA: Kluwer, 1996.

[18] G. Wang, K. Xiao, and X.-G. Xia, *Performance analysis of precoded OFDM systems in frequency-selective multipath fading channels*, 1999, preprint.

[19] *CISCO, VOFDM*, http://www.cisco.com/warp/public/cc/pd/witc/wt2700/mulpt_wp.htm.

[20] J.-C. Guey, M. P. Fitz, M. R. Bell, and W.-Y. Kuo, "Signal design for transmitter diversity wireless communication systems over Rayleigh fading channels," *IEEE Trans. Commun.*, vol. 47, pp. 527–537, Apr. 1999.

[21] V. Tarokh, N. Seshadri, and A. R. Calderbank, "Space–time codes for high data rate wireless communication: Performance criterion and code construction," *IEEE Trans. Inform. Theory.*, vol. 44, pp. 744–765, Mar. 1998.

[22] V. Tarokh, H. Jafarkani, and A. R. Calderbank, "Space–time block codes from orthogonal designs," *IEEE Trans. Inform. Theory*, vol. 45, pp. 1456–1467, Sept. 1999.

[23] T. L. Marzetta and B. M. Hochwald, "Capacity of a mobile multiple-antenna communication link in Rayleigh flat fading," *IEEE Trans. Inform. Theory*, vol. 45, pp. 139–157, Jan. 1999.

[24] B. M. Hochwald and W. Sweldens, "Differential unitary space–time modulation," *IEEE Trans. Commun.*, vol. 48, pp. 2041–2052, Dec. 2000.

[25] B. L. Hughes, "Differential space–time modulation," *IEEE Trans. Inform. Theory*, vol. 46, pp. 2567–2578, Nov. 2000.

[26] B. Lu and X.-D. Wang, "Space–time code design in OFDM systems," in *Proc. GLOBECOM 2000*, San Francisco, CA, Nov. 27–Dec. 1, 2000.

[27] D. Agrawal, V. Tarokh, A. Naguib, and N. Seshadri, "Space–time coded OFDM for high data-rate wireless communication over wideband channels," in *Proc. IEEE Vehicular Technology Conf.*, vol. 3, Ottawa, ON, Canada, May 1998, pp. 2232–2236.

[28] X.-B. Liang and X.-G. Xia, "Some unitary signal constellations for differential space–time modulation," in *Proc. Asilomar Conf.*, Pacific Grove, CA, Oct. 31–Nov. 2, 2000.

Xiang-Gen Xia (M'97–SM'00) received the B.S. degree in mathematics from Nanjing Normal University, Nanjing, China, the M.S. degree in mathematics from Nankai University, Tianjin, China, and the Ph.D. degree in electrical engineering from the University of Southern California, Los Angeles, in 1983, 1986, and 1992, respectively.

He was a Lecturer at Nankai University, Tianjin, China, from 1986 to 1988, a Teaching Assistant at the University of Cincinnati from 1988 to 1990, a Research Assistant at University of Southern California from 1990 to 1992, and a Research Scientist at the Air Force Institute of Technology from 1993 to 1994. He was a Senior/Research Staff Member at Hughes Research Laboratories, Malibu, CA, from 1995 to 1996. In September 1996, he joined the Department of Electrical and Computer Engineering, University of Delaware, Newark, DE, where he is currently an Associate Professor. His current research interests include communication systems including equalization and coding, SAR and ISAR imaging of moving targets, wavelet transform and multirate filterbank theory and applications, time-frequency analysis and synthesis, and numerical analysis and inverse problems in signal/image processing. He is the author of the book *Modulated Coding for Intersymbol Interference Channels* (New York: Marcel Dekker, 2000).

Dr. Xia is a member of the Signal Processing for Communications Technical Committee in the IEEE Signal Processing Society. He is currently an Associate Editor of the IEEE TRANSACTIONS ON SIGNAL PROCESSING and the AURASIP *Journal of Applied Signal Processing*, as well as Guest Editor of Space–Time Coding and Its Applications in the AURASIP *Journal of Applied Signal Processing*. He received the National Science Foundation (NSF) Faculty Early Career Development (CAREER) Program Award in 1997 and the Office of Naval Research (ONR) Young Investigator Award in 1998.